A physiological effective connectome of the human brain, based on intracranial electrical stimulation

P 0501

Cristian Donos[1], Mihai Maliia[2], Ioana Mindruta[2,3], Jean Ciurea[4], Laura Craciun[2], Andrei Barborica[1,5]

[1]Physics Department, University of Bucharest, Bucharest, Romania, [2]Neurology Department, University Emergency Hospital, Bucharest, Romania,

[3]Neurology Department, Carol Davila University of Medicine and Pharmacy, Bucharest, Romania, [4]Neurosurgery Department, Bagdasar-Arseni Hospital, Bucharest, Romania, [5]FHC Inc, Bowdoin ME, USA

Introduction

Several MRI and DTI methods already delivered a whole brain structural connectome [1], however none of them are able to directly probe the causal functional (*effective*) brain connectivity using native electrical signaling. The study of cortico-cortical evoked potentials using high-density stereoelectroencephalographic (SEEG) recordings represents perhaps the most direct way of exploring brain connectivity. However, SEEG investigations are limited to the patients with drug-resistant epilepsy, which may present disrupted connectivity patterns [2,3]. In order to dissociate pathological from physiological connectivity, we propose a method that combines individual patient's connectivity with saliency maps and epileptogenicity of the cortical areas calculated retrospectively on a larger patient dataset.

Methods

24 patients with refractory epilepsy (Table 1) were implanted with depth electrodes for presurgical evaluation. Single pulse electrical stimulation, using biphasic pulses with 3ms pulse duration and current intensity in the 0.25-5mA range was applied to each pair of adjacent contacts and responses evoked by stimulation were recorded from other contacts located in remote brain areas. We calculated the RMS value over the 10-110 ms interval after each stimulation pulse. We considered that a contact is activated by stimulation if the responses are correlated with the stimulation current (Spearman's r>0.5, p<0.05) and the mean RMS value across all stimulation pulses in a trial is higher than the 3rd quartile value (Q3) of all the responses recorded within a patient [4]. Responses from the activated contacts were weighted by the epileptogencity of each area and averaged for each patient. Further weighting was performed by calculating the saliency of each non-pathological connection in the patient database. We use the terms "inbound" and "outbound" to illustrate the connections ending on and starting from each brain structure, respectively.

Patient	Sex	Age	Epilepsy	Lateralisation	Localization	Pathology	MRI Lesion	Number of electrodes	Number of contacts	RMS Q3 (uV)	Surgical Outcome
1	F	17	Frontal	Left	Premotor dorsolateral	Type II BFCD	Negative	11	104	95.8	Engel IIIB
2	M	39	Occipital	Left	Occipito-temporal basal	Polimycrogyria	MCD	16	194	61.3	Engel IA
3	M	47	Temporal	Left	Middle temporal gyrus	DNET	DNET	11	101	87.7	Engel II
4	F	40	Prefrontal	Left	Prefrontal	Type II BFCD	Type II BFCD	11	141	89.6	Engel IA
5	F	35	Mesio-temporal	Right	Amygdala	Temporal sclerosis	Negative	12	160	56.4	Engel IIB
6	F	24	Fronto-xentral	Right	Rolandic	Type II A FCD	Type II FCD	15	138	63.9	Engel IB
7	M	24	Occipital	Right	Occipito-temporal basal	Typa I FCD	MCD	14	157	25.3	Engel IIIB
8	F	25	Temporal	Right	Amygdala	Type I FCD	Type II FCD	10	111	62.5	Engel IIB
9	F	46	Temporal	Right	Temporal pole	Type II BFCD	Type II FCD	9	102	106.5	Engel IIIB
10	M	33	Frontal	Left	Mesial prefrontal	Type I B FCD	Type I FCD	17	174	48.4	Engel IA
11	F	11	Frontal	Right	Mesial and lateral premotor	Type II A FCD	Misleading-type II B - like FCD in temporal operculum	9	183	77.7	Engel IA
12	F	9	Frontal	Right	Lateral prefrontal	Type II A FCD	Type II FCD	13	180	54.8	Engel IC
13	F	35	Frontal	Right	Middle cingulate	Not available (thermocoagulation)	Negative	14	169	48.2	Engel IA
14	M	28	Temporal	Right	Temporal	Type I FCD	Type I FCD	17	188	52.1	Engel IA
15	F	25	Bitemporal	Bilateral	Bitemporal	Type I FCD	Negative	17	219	51.8	Engel IB
16	F	36	Opercular	Right	Parietal-temporal, posterior operculum	Type II BFCD	Type II FCD	15	205	91.4	Engel IA
17	F	42	Temporal plus	Right	Temporal pole and temporo-mesial	Type I FCD	Hippocampal atrophy	14	205	72.1	Engel IA
18	F	37	Temporal	Left	Temporal pole and temporo-mesial	Type IIA FCD	Negative	13	160	43.6	Engel IA
19	M	26	Occipital	Bilateral	Biocipital	Not operated on	Negative	14	211	73.3	-
20	M	53	Frontal	Left	Frontal pole	Cavernoma	Multiple cavernomas	11	166	30.2	Engel IA
21	M	39	Bitemporal	Bilateral	Bitemporal	Not operated on	Negative	11	167	44.9	-
22	F	42	Temporal	Left	Temporal	Not available	Hippocampal atrophy and left superior temporal gyrus malformation	11	147	58.8	Engel IA
23	M	42	Mesio-Temporal	Left	Occipito-temporo basal	Type II A FCD	Left hippocampal sclerosis and superior temporal gyrus dysplasia	14	194	65.2	Engel IB
24	M	29	Frontal	Right	Premotor	Type II BFCD	Type II BFCD	9	112	72	Engel IA

Table 1. Patients participating in our study.

The directionality of the connections between a pair of structures (A, B) is evidenced by the asymmetry in responses $R_{A\to B}$, $R_{B\to A}$ to sequential stimulation of each structure. A directionality factor $DF_{A\leftrightarrow B}$ has been defined as:

$$DF_{A\leftrightarrow B} = \left|\frac{R_{A\to B} - R_{B\to A}}{R_{A\to B} + R_{B\to A}}\right|$$

Abbrev	Structure's name	Contacts		Patients		Abbrev	Structure's name	Contacts		Patients	
		Right	Left	Right	Left			Right	Left	Right	Left
	FRONTAL						OPERCULAR-INSULAR				
ACC	Anterior Cingulate Cortex	13	13	6	6	ai	Anterior Insula	8	2	5	1
DLPFC	Dorso-Lateral Prefrontal Cortex	24	5	5	3	OpF	Operculum Frontalis	5	6	3	3
DMPFC	Dorso-Mesial Prefrontal Cortex	4	8	2	3	OpP	Operculum Parietalis	17	10	4	4
MCC	Middle Cingulate Gyrus	8	2	3	1	OpR	Operculum Rolandis	9	2	4	1
MOFC	Mesial Orbito-Frontal Cortex	4	8	2	4	OpT	Operculum Temporalis	14	15	5	5
OF	Orbito-Frontal	10	8	4	4	pi	Posterior Insula	18	16	7	7
PMC	Premotor Cortex	24	9	6	2		PARIETAL				
preSMA	Pre-Supplementary Motor Area	3	1	2	1	IPL	Inferior Parietal Lobule	24	7	7	5
R	Precentral Gyrus	18	12	6	3	PCC	Posterior Cingulate Cortex	7	21	4	8
SMA	Supplementary Motor Area	4	2	2	1	PCL	Paracentral Lobule	12	6	4	3
VLPFC	Ventro-Lateral Prefrontal Cortex	4	11	2	3	PrC	Precuneus	6	12	3	4
VMPFC	Ventro-Mesial Prefrontal Cortex	0	2	0	1	S	Postcentral Gyrus	7	2	4	1
	TEMPORAL					SPL	Superior Parietal Lobule	8	21	4	6
A	Amygdala	10	12	4	5		OCCIPITAL				
E	Entorhinal	0	4	0	2	C	Cuneus	2	0	1	0
F	Fusiform Gyrus	6	20	3	6	LG	Lingual Gyrus	17	13	6	5
Hi	Hippocampus	7	3	4	1	O	Lateral Occipital	3	5	2	1
ITG	Inferior Temporal Gyrus	20	21	9	7	TPO	Temporo-Parieto-Occipital Junction	16	4	6	1
MTG	Middle Temporal Gyrus	18	26	6	6	V1	Primary Visual Cortex	5	1	1	1
PHG	Parahippocampal Gyrus	4	19	2	4		SUBCORTICAL				
STG	Superior Temporal Gyrus	13	21	5	7	BG	Basal Ganglia	0	2	0	2
TP	Temporal Pole	3	6	2	2	Th	Thalamus	0	2	0	1

Table 2. List of all structures implanted in our patient lot.

Results

Over the 24 patient set, we have inserted a total of 13 ± 2.5 depth electrodes, probed 609 sites using electrical stimulation and recorded 36980 responses in 1481 locations. A number of 9448 (25.5%) recorded responses met our amplitude and correlation with stimulus criteria and were used for calculating the physiological effective connectome (Figure 1).

The physiological effective connectome contains 70 brain structures from both hemispheres and has a mean directionality factor (DF) ± SD of 0.63 ± 0.40.

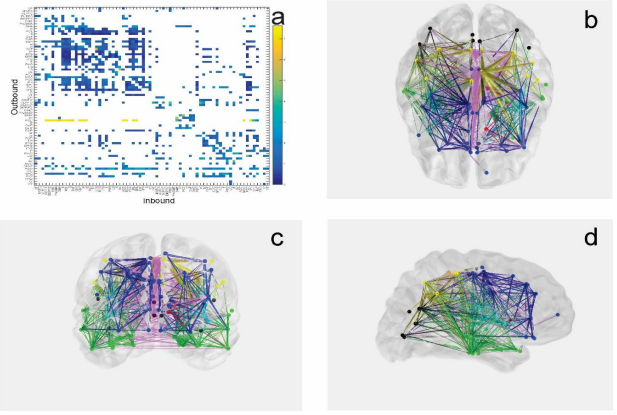

Figure 1. The physiological effective connectome. a) 2D representation as an adjacency matrix, in which the normalized responses between two structures are color-coded. b),c),d) Axial, coronal, and sagittal views of the 3D frustums representation. For each connection, the large base of the frustum, whose radius is directly proportional with the normalized RMS response, indicate the stimulation structure, while the small base indicate the structure in which the response was recorded.

The effective connectivity of 8 brain structures relevant to temporal lobe epilepsy is shown in Figure 2.

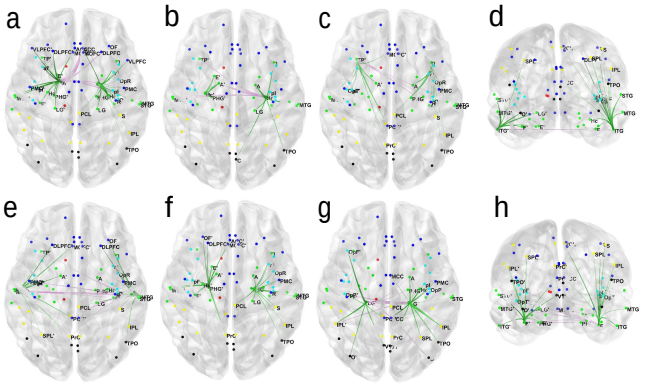

Figure 2. The physiological effective connectivity of temporal lobe structures in 3D frustums representation. a) amygdala, b) hippocampus, c) temporal pole, d) inferior temporal gyrus, e) middle temporal gyrus, f) parahippocampal gyrus, g) lingual gyrus, h) fusiform gyrus.

Conclusions

Using direct electrical stimulation, we obtained a physiological effective connectome covering a 70 brain structures from both hemispheres.

There was a significant directionality in the functional connections between structures.

This data can be used as reference tool for planning the SEEG implantations and for differential analysis of altered versus normal brain connectivity in epileptic patients.

Acknowledgments

Supported by Romanian government UEFISCDI research grant PN-II-ID-PCE-2011-3-0240

References

1. Yeh FC, Tseng WY. NTU-90: a high angular resolution brain atlas constructed by q-space diffeomorphic reconstruction. Neuroimage. 2011 Sep 1; 58(1):91-9.
2. Lee HW, Arora J, Papademetris X, Tokoglu F, Negishi M, Scheinost D, Farooque P, Blumenfeld H, Spencer DD, Constable RT. Altered functional connectivity in seizure onset zones revealed by fMRI intrinsic connectivity. Neurology. 2014 Dec 9; 83(24):2269-77.
3. Liao W, Zhang Z, Pan Z, Mantini D, Ding J, Duan X, Luo C, Lu G, Chen H. Altered functional connectivity and small-world in mesial temporal lobe epilepsy. PLoS One. 2010 Jan 8;5(1):e8525.
4. Donos C, Mîndruţă I, Ciurea J, Măliia MD, Barborica A. A comparative study of the effects of pulse parameters for intracranial direct electrical stimulation in epilepsy. Clin Neurophysiol. 2015 Mar 2. pii: S1388-2457(15)00118-2.